

Electronic Supplementary Information for
**Azo-bridged Covalent Porphyrinic Polymers (Azo-CPPs): Synthesis and CO₂ Capture
properties†**

Liming Tao^a, Fang Niu^b, Di Zhang^a, Tingmei Wang^a and Qihua Wang^{*a}

^a *State Key Laboratory of Solid Lubrication, Lanzhou Institute of Chemical Physics, Chinese
Academy of Sciences, Lanzhou, Gansu 730000, P.R. China. Fax: 86 0931 4968252; Tel: 86 0931
4968252*

^b *College of Chemistry and Chemical Engineering, Lanzhou University, Lanzhou, Gansu 730000,
P.R. China. E-mail: niufang@lzu.edu.cn.*

Corresponding to: qhwang@licp.cas.cn.

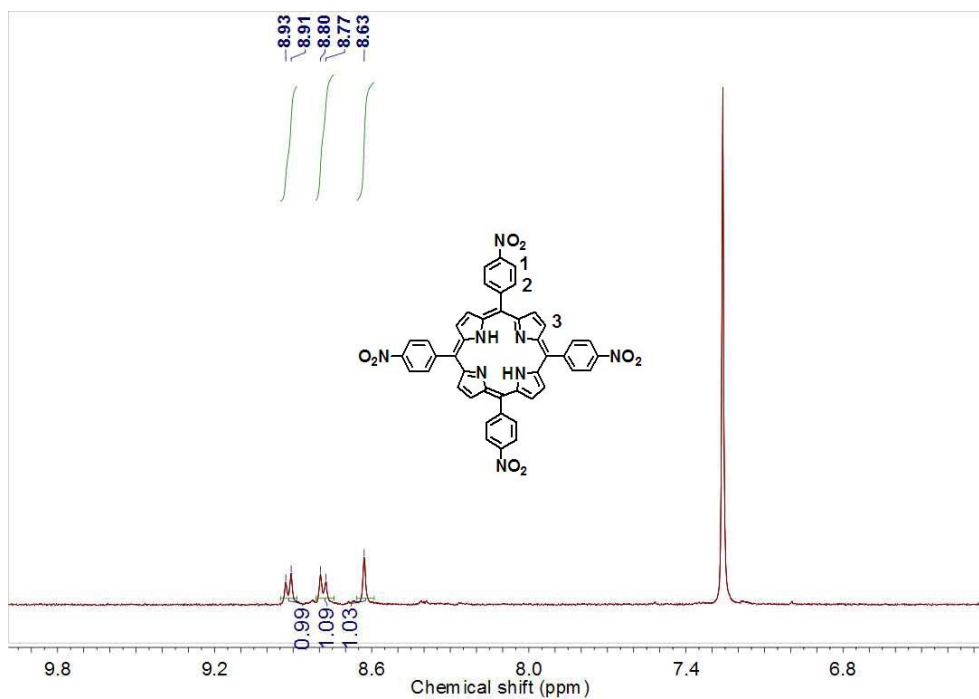


Fig. S1 ^1H NMR spectrum of 4NO₂TPP (CDCl₃, 400 MHz)

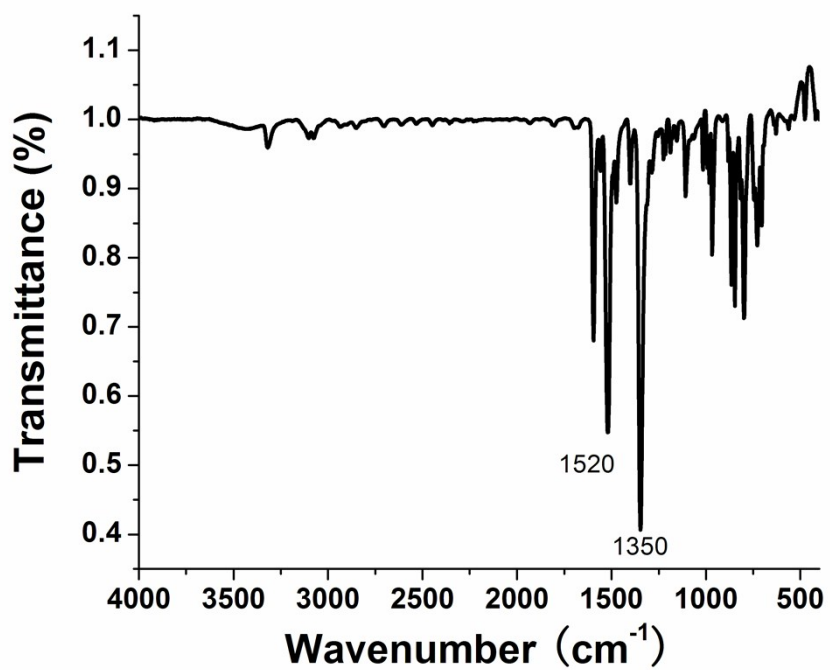


Fig. S2 FT-IR spectrum of 4NO₂TPP (KBr pellets)

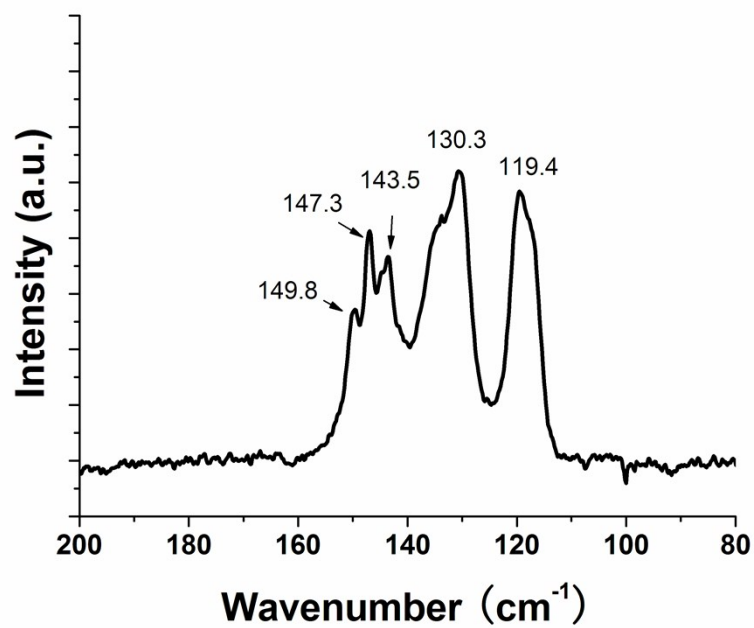


Fig. S3 Solid-state ^{13}C NMR spectrum of 4NO₂TPP (100 MHz)

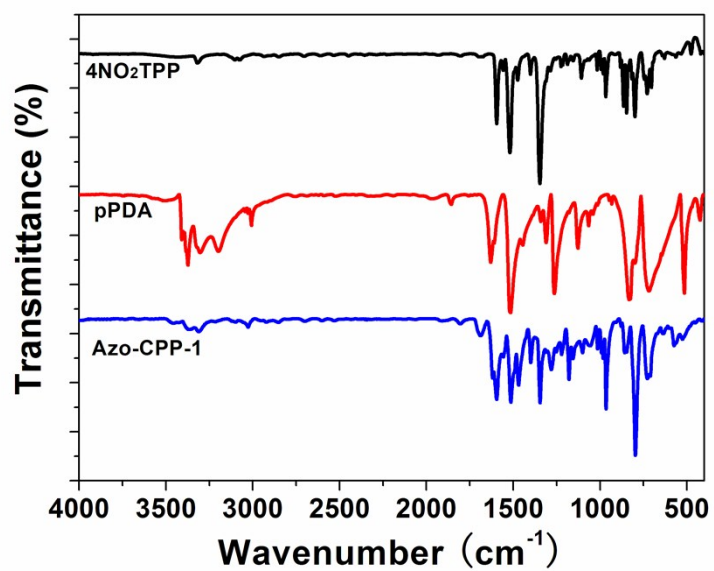


Fig. S4 FTIR spectra comparison of Azo-CPP-1 and the monomers (KBr pellets)

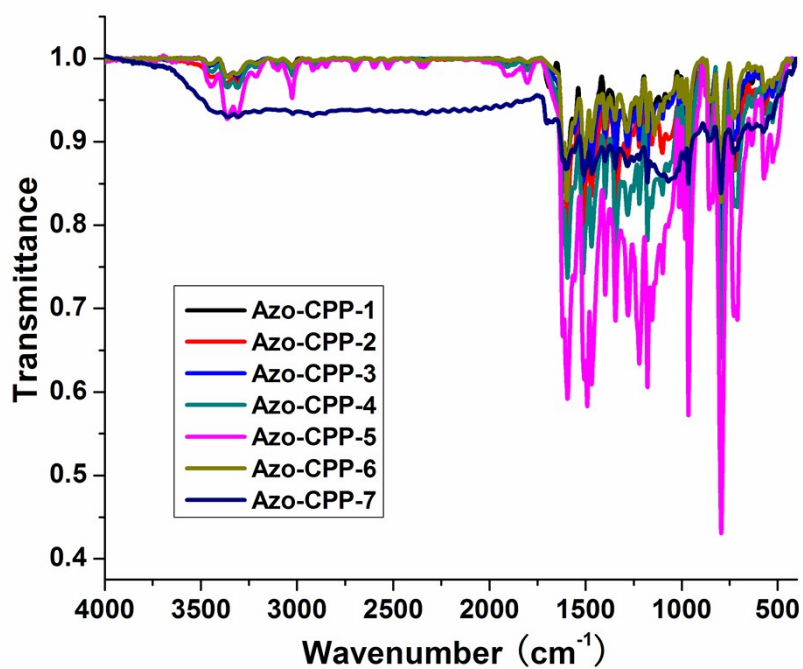


Fig. S5 FT-IR spectra of the Azo-CPPs. (KBr pellets)

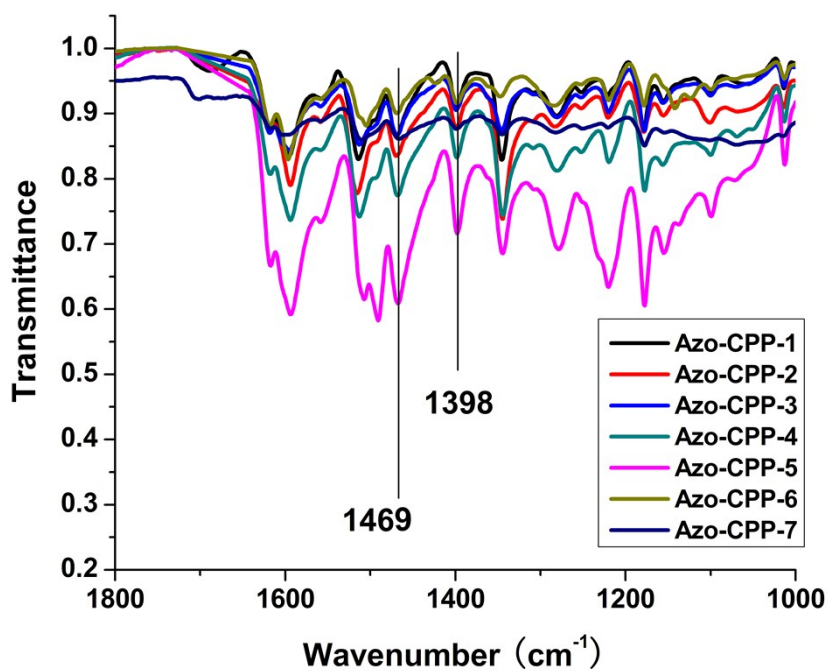


Fig. S6 FT-IR spectra of the Azo-CPPs, expanded between 1800 ~ 1000 cm⁻¹. (KBr pellets)

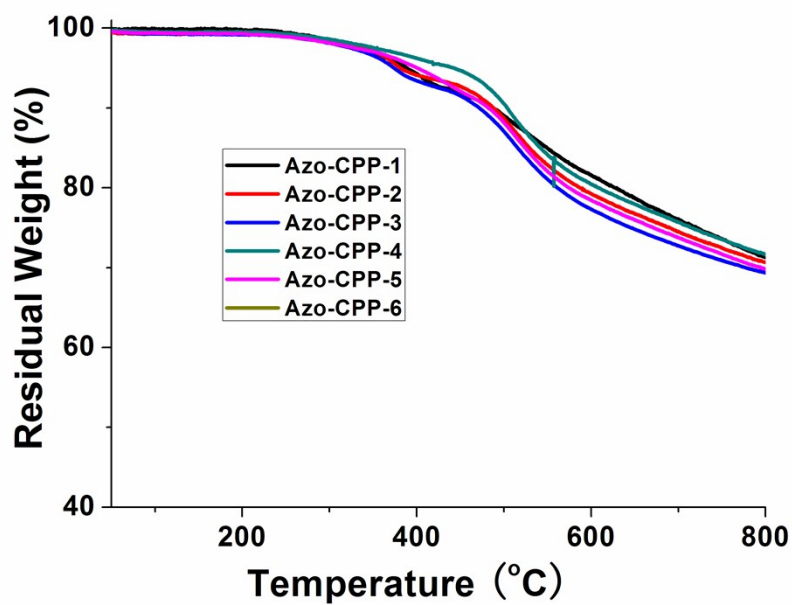


Fig. S7 TGA curves of Azo-CPPs. (N_2 , $10\text{ }^\circ\text{C}/\text{min}$)

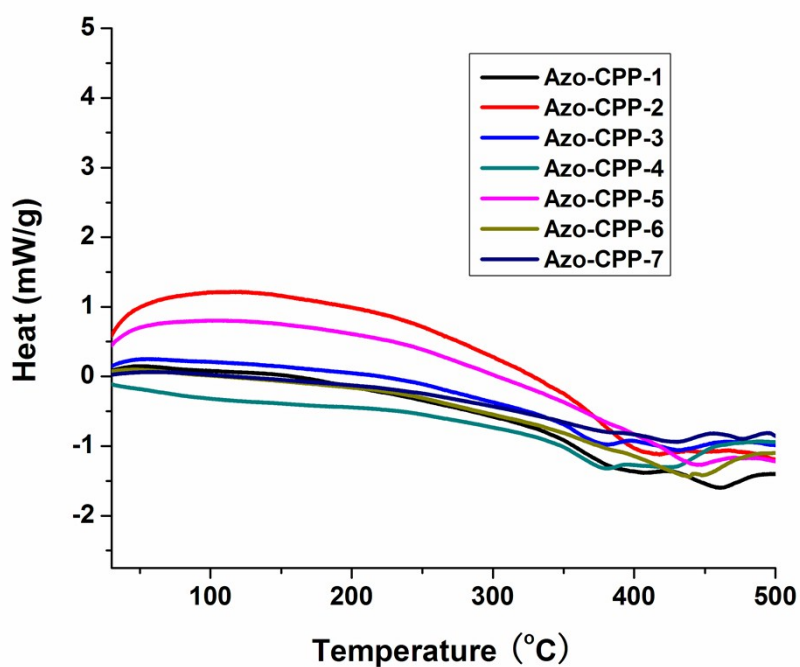


Fig. S8 DSC curves of the Azo-CPPs. ($10\text{ }^\circ\text{C}/\text{min}$, N_2)

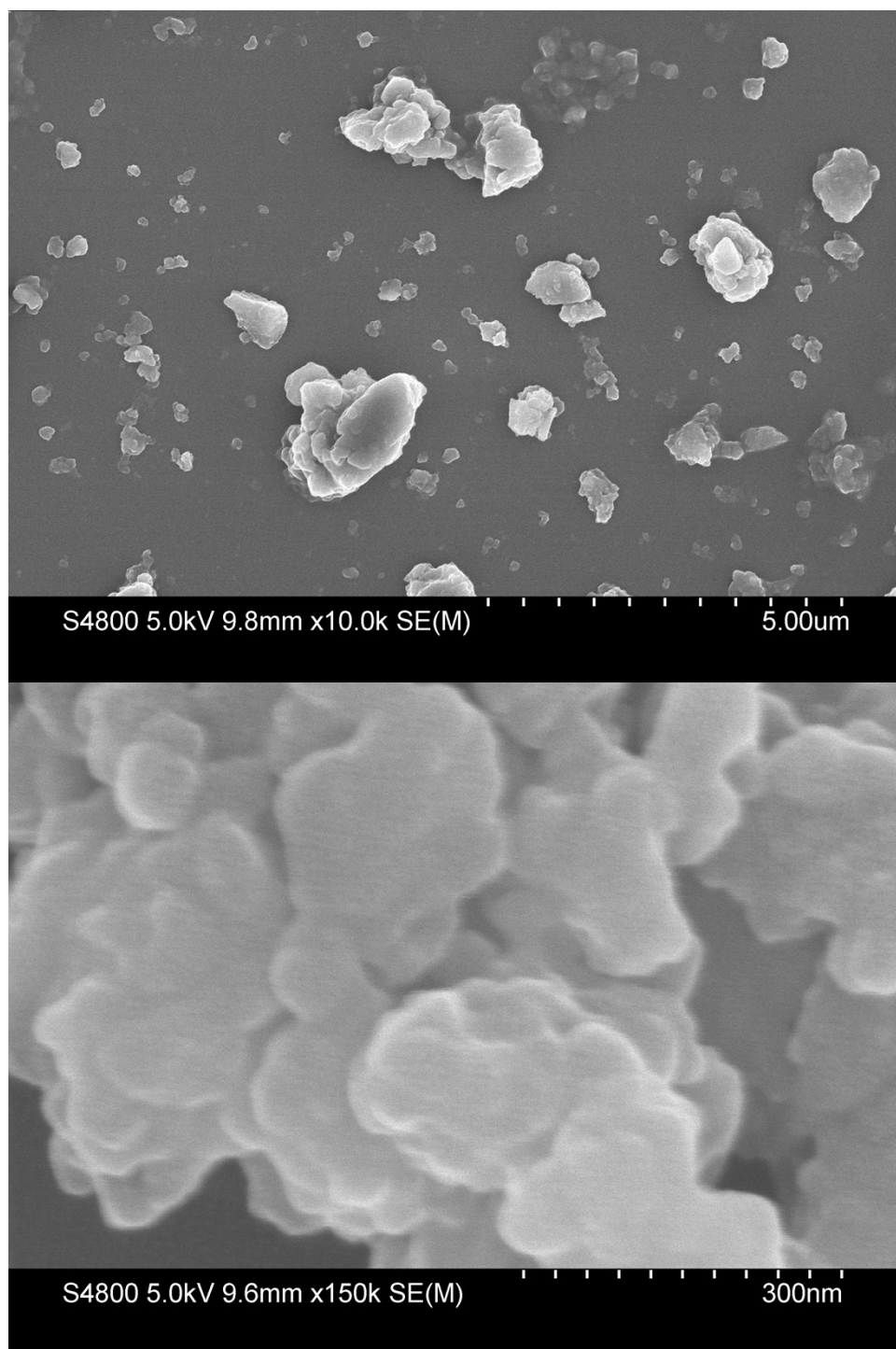


Fig. S9 SEM images of Azo-CPP-1

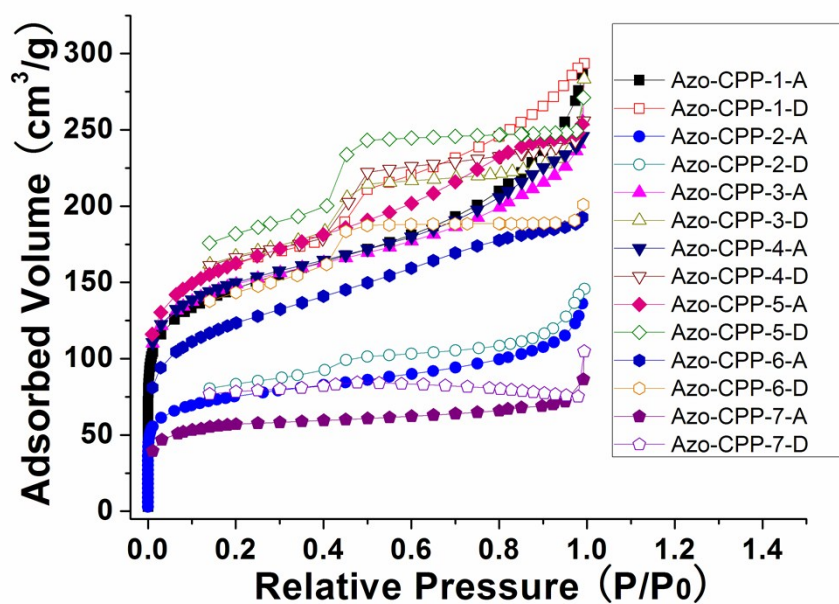


Fig. S10 Nitrogen adsorption and desorption isotherms at 77.3 K for all Azo-CPPs.

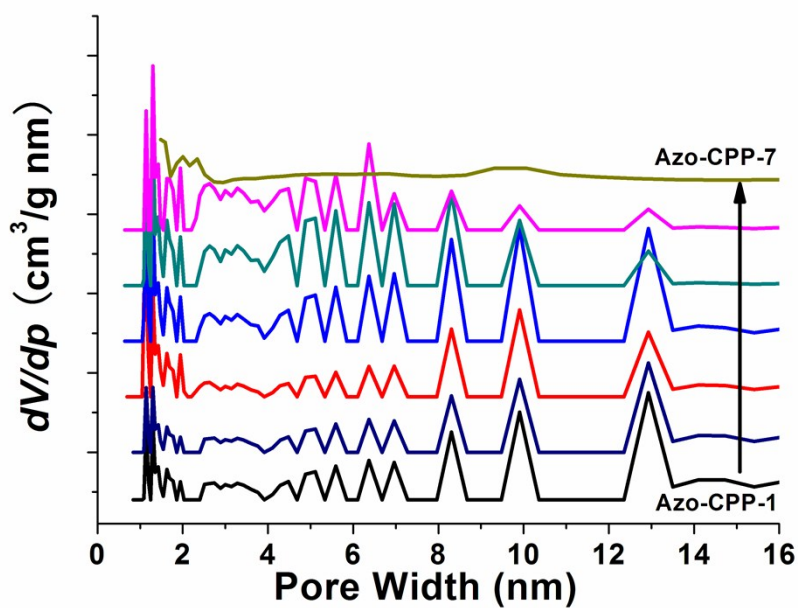


Fig. S11 Pore size distributions (PSD) calculated by the NLDFT method for all Azo-CPPs.

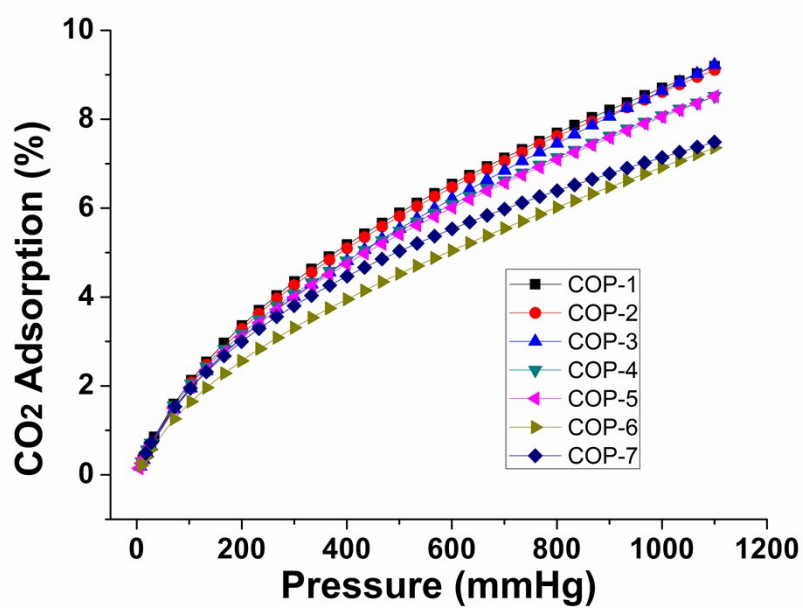


Fig. S12 CO₂ adsorption isotherms at 273 K for all Azo-CPPs.

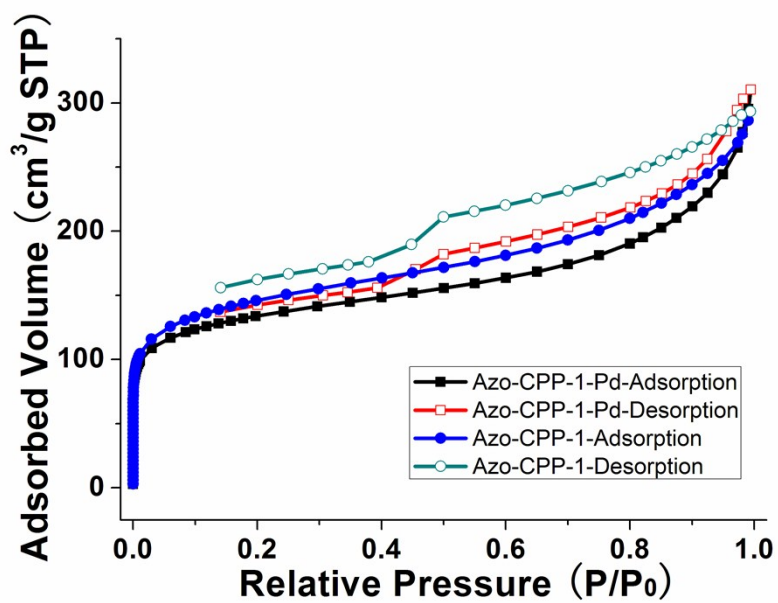


Fig. S13 Nitrogen adsorption and desorption isotherms at 77.3 K for Azo-CPP-1 and Azo-CPP-1-Pd.

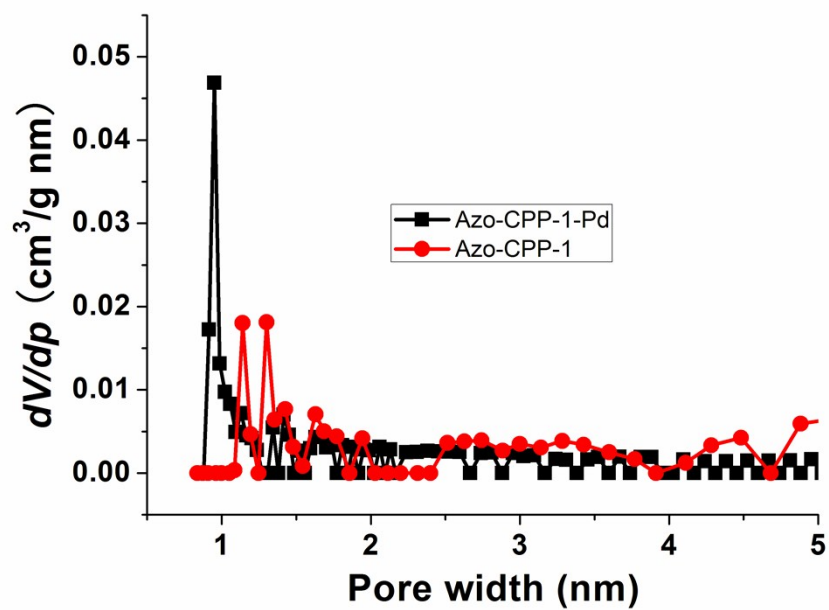


Fig. S14 Pore size distributions (PSD) calculated by the NLDFT method for Azo-CPP-1 and Azo-CPP-1-Pd.

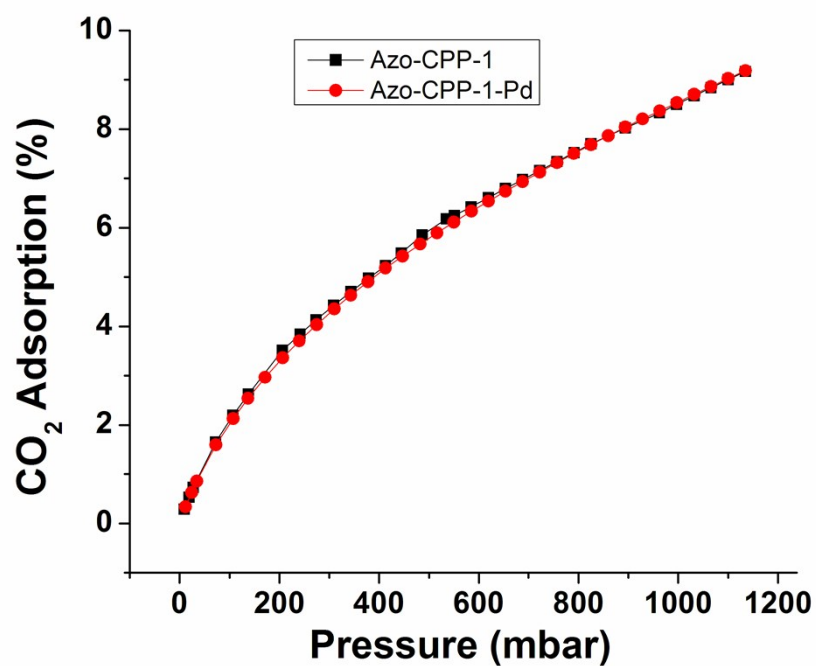


Fig. S 15 CO₂ adsorption isotherms at 273 K for Azo-CPP-1 and Azo-CPP-1-Pd

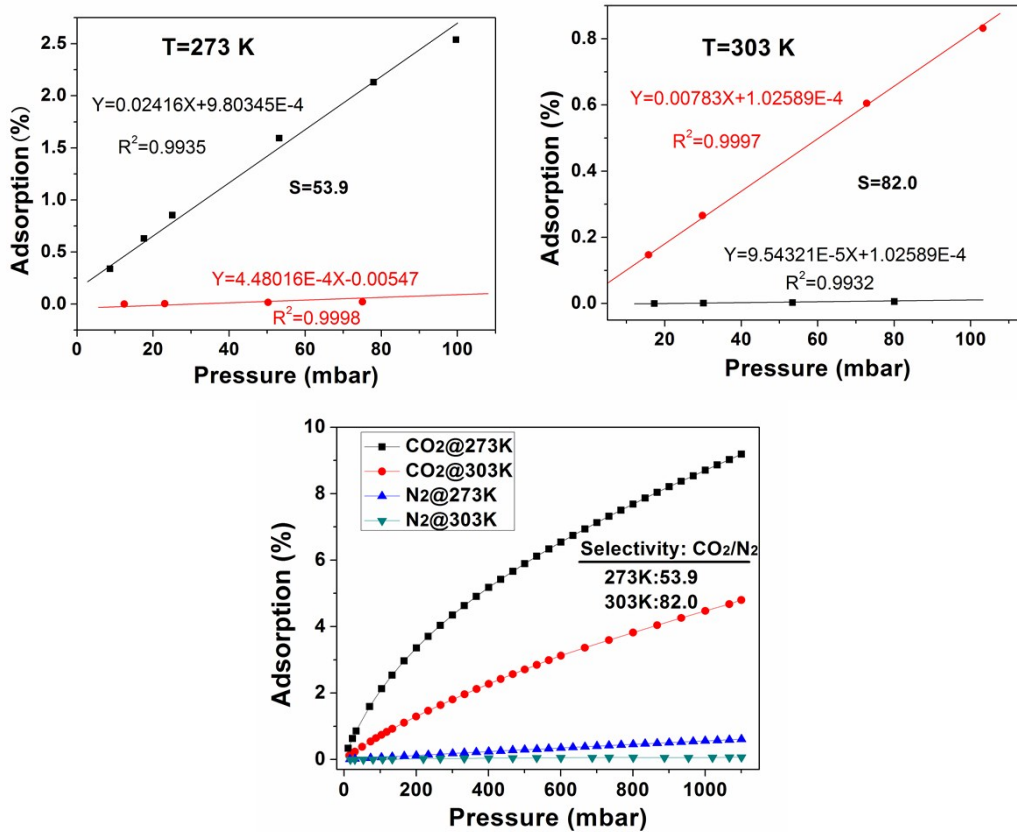


Fig. S16 CO₂/N₂ selectivities for Azo-CPP-1 calculated using the Henry's Law constants in the linear low pressure range (0~100 mbar).

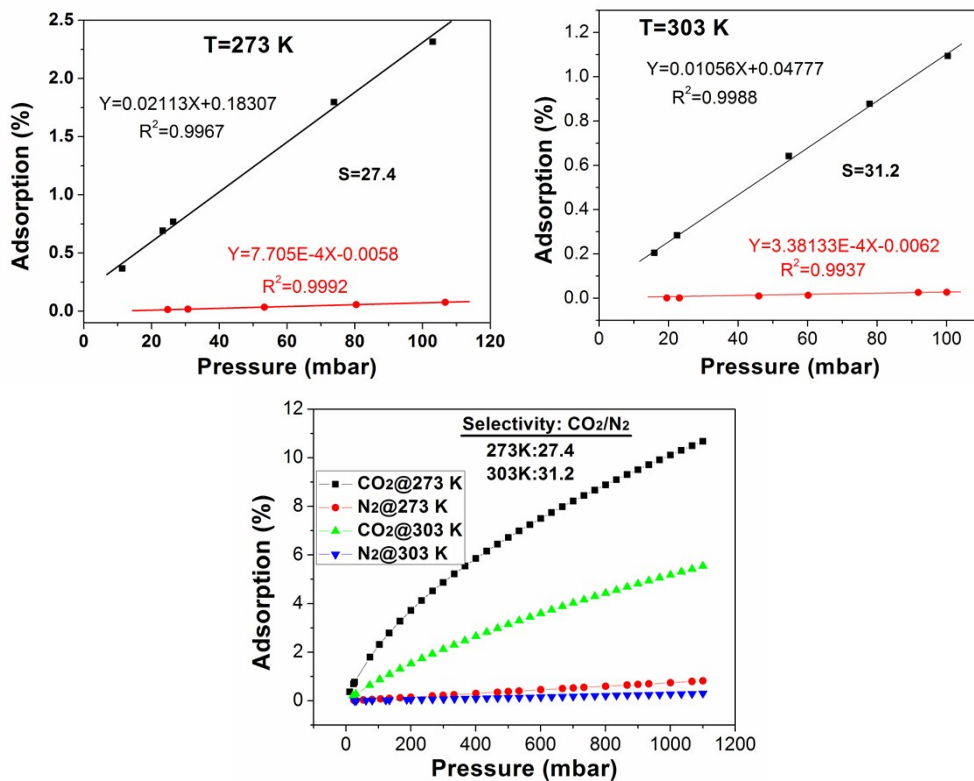


Fig. S17 CO₂/N₂ selectivities for Azo-CPP-2 calculated using the Henry's Law constants in the linear low pressure range (0~100 mbar)

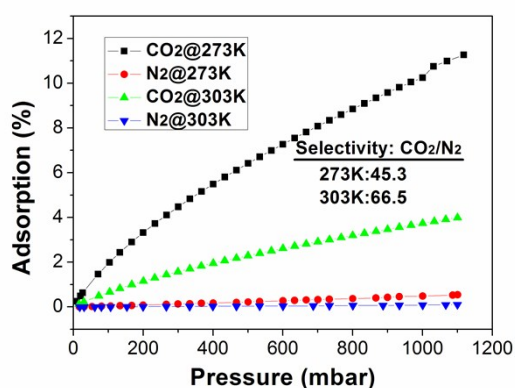
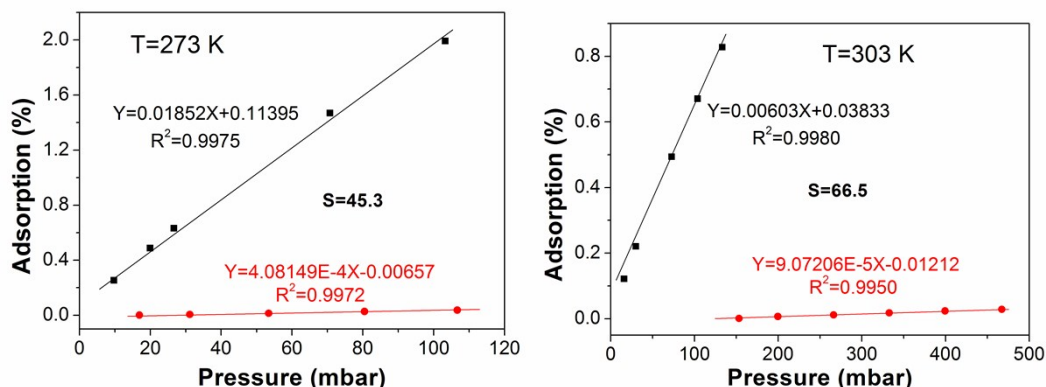


Fig. S18 CO₂/N₂ selectivities for Azo-CPP-3 calculated using the Henry's Law constants in the linear low pressure range (0~100 mbar). Due to the very low adsorption of N₂ at 303 K in the range of 0~100 mbar, the data from 150 to 500 mbar were used instead.

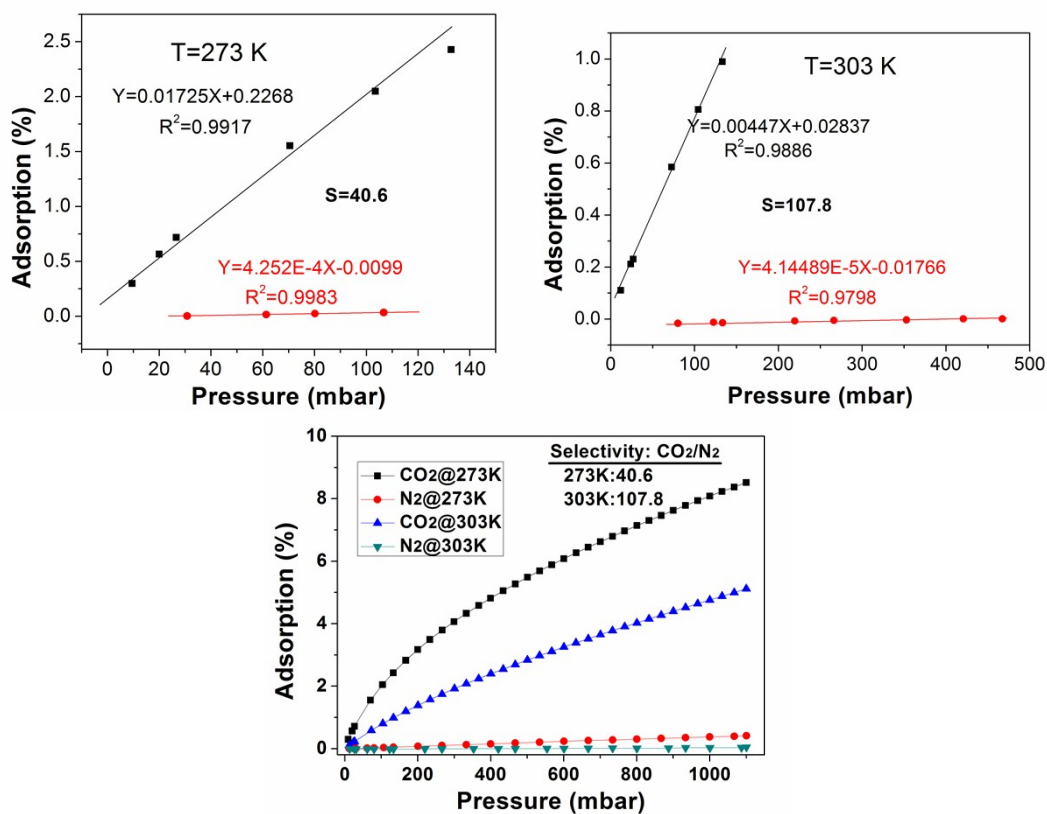


Fig. S19 CO₂/N₂ selectivities for Azo-CPP-4 calculated using the Henry's Law constants in the linear low pressure range (0~100 mbar). Due to the very low adsorption of N₂ at 303 K in the range of 0~100 mbar, the data from 90 to 500 mbar were used instead.

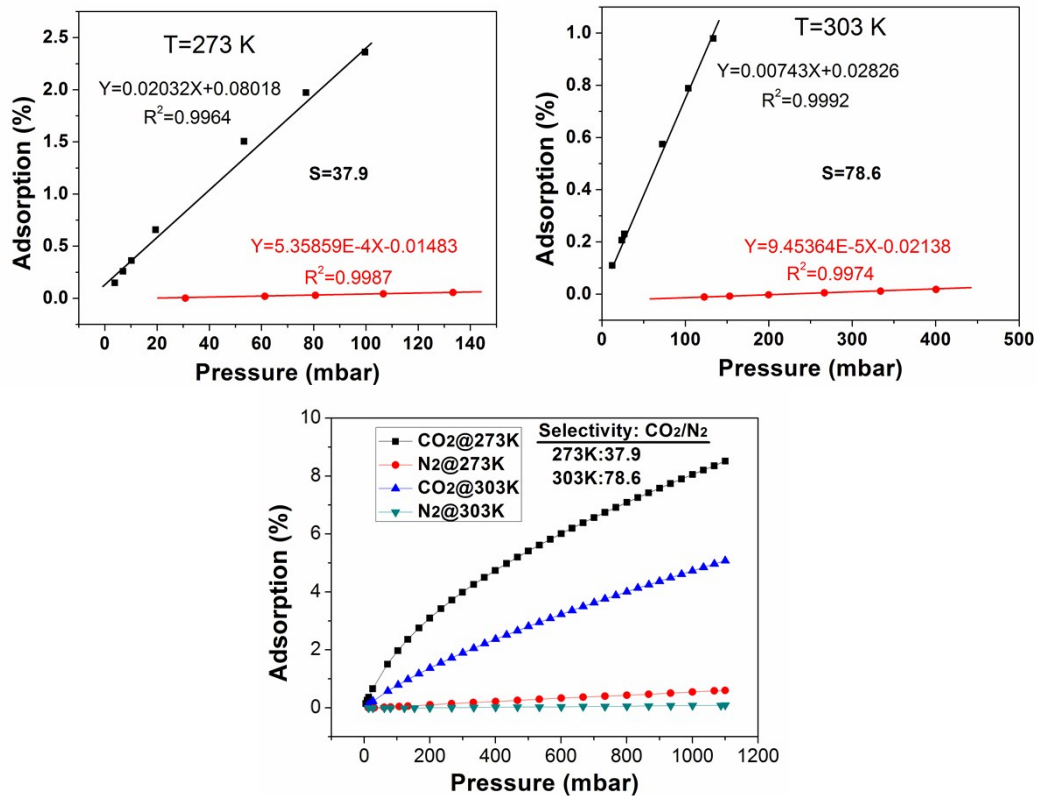
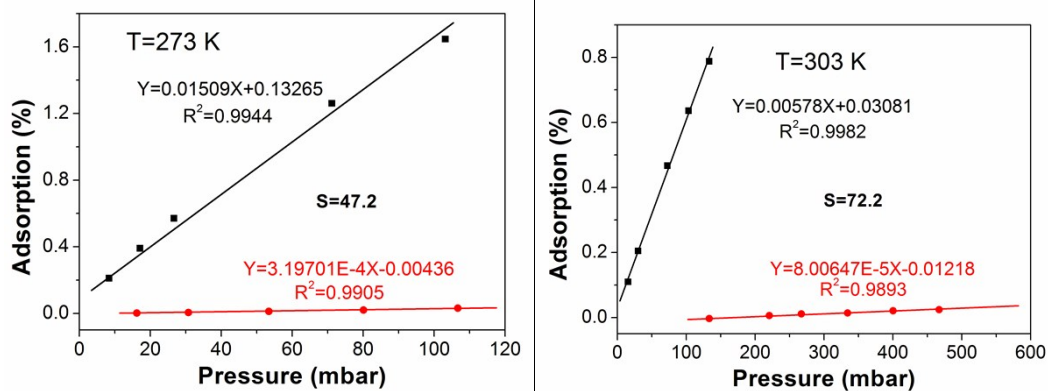


Fig. S20 CO₂/N₂ selectivities for Azo-CPP-5 calculated using the Henry's Law constants in the linear low pressure range (0~100 mbar). Due to the very low adsorption of N₂ at 303 K in the range of 0~100 mbar, the data from 100 to 500 mbar were used instead.



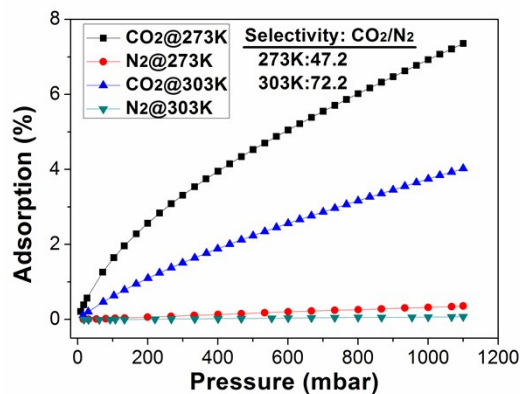


Fig. S21 CO₂/N₂ selectivities for Azo-CPP-6 calculated using the Henry's Law constants in the linear low pressure range (0~100 mbar). Due to the very low adsorption of N₂ at 303 K in the range of 0~100 mbar, the data from 100 to 500 mbar were used instead.

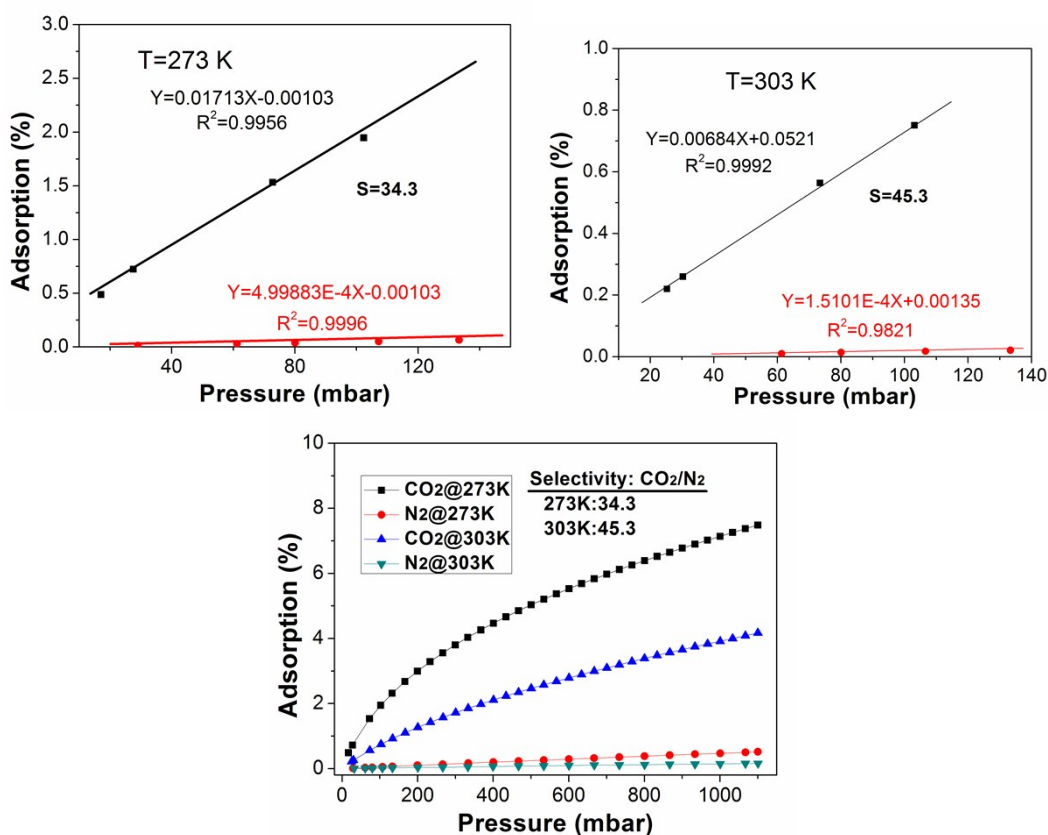


Fig. S22 CO₂/N₂ selectivities for Azo-CPP-7 calculated using the Henry's Law constants in the linear low pressure range (0~150 mbar).